Ultra-broadband one-to-two wavelength conversion using low-phase-mismatching four-wave mixing in silicon waveguides

Shiming Gao,[1,2*] En-Kuang Tien,[2] Qi Song,[2] Yuewang Huang,[2] and Ozdal Boyraz[2]

[1] *Centre for Optical and Electromagnetic Research, State Key Laboratory of Modern Optical Instrumentation, Zhejiang University, Hangzhou 310058, China*

[2] *Advanced Photonics Device and System Laboratory, Department of Electrical Engineering and Computer Science, University of California, Irvine, California 92697, USA*

**gaosm@zju.edu.cn*

Abstract: An ultra-broadband wavelength conversion is presented and experimentally demonstrated based on nondegenerate four-wave mixing in silicon waveguides. Two idlers can be generated and their wavelengths can be freely tuned by using two pumps where the first pump is set close to the signal and the second pump is wavelength tunable. Using this scheme, a small phase-mismatch and hence an ultra-broad conversion bandwidth is realized in spite of the waveguide dispersion profile. We show that the experimental demonstrations are consistent with the theoretical estimations. Total conversion bandwidth is estimated to reach >500 nm and it can provide a feasible approach to realize one-to-two wavelength conversion among different telecommunication bands between 1300 nm and 1800 nm.

OCIS codes: (190.4380) Nonlinear optics, four-wave mixing; (190.4390) Nonlinear optics, integrated; (130.7405) Wavelength conversion devices.

References and links

1. S. J. B. Yoo, "Wavelength conversion technologies for WDM network applications," J. Lightwave Technol. **14**(6), 955–966 (1996).
2. M. Nakamura, H. Ueda, S. Makino, T. Yokotani, and K. Oshima, "Proposal of networking by PON technologies for full Ethernet services in FTTx," J. Lightwave Technol. **22**(11), 2631–2640 (2004).
3. S. Gao, C. Yang, and G. Jin, "Flat broad-band wavelength conversion based on sinusoidally chirped optical superlattices in lithium niobate," IEEE Photon. Technol. Lett. **16**(2), 557–559 (2004).
4. R. Jiang, R. Saperstein, N. Alic, M. Nezhad, C. McKinstrie, J. Ford, Y. Fainman, and S. Radic, "Parametric wavelength conversion from conventional near-infrared to visible band," IEEE Photon. Technol. Lett. **18**(23), 2445–2447 (2006).
5. S. Gao, C. Yang, X. Xiao, Y. Tian, Z. You, and G. Jin, "Bandwidth enhancement and response flattening of cascaded sum- and difference-frequency generation-based wavelength conversion," Opt. Commun. **266**(1), 296–301 (2006).
6. Z. G. Lu, P. J. Bock, J. R. Liu, F. G. Sun, and T. J. Hall, "All-optical 1550 to 1310 nm wavelength converter," Electron. Lett. **42**(16), 937–938 (2006).
7. H. Rong, Y.-H. Kuo, A. Liu, M. Paniccia, and O. Cohen, "High efficiency wavelength conversion of 10 Gb/s data in silicon waveguides," Opt. Express **14**(3), 1182–1188 (2006), http://www.opticsinfobase.org/oe/abstract.cfm?URI=OPEX-14-3-1182.
8. B. G. Lee, A. Biberman, A. C. Turner-Foster, M. A. Foster, M. Lipson, A. L. Gaeta, and K. Bergman, "Demonstration of broadband wavelength conversion at 40 Gb/s in silicon waveguides," IEEE Photon. Technol. Lett. **21**(3), 182–184 (2009).
9. S. Gao, X. Zhang, Z. Li, and S. He, "Polarization-independent wavelength conversion using an angled-polarization pump in a silicon nanowire waveguide," IEEE J. Sel. Top. Quantum Electron. **16**(1), 250–256 (2010).
10. H. Fukuda, K. Yamada, T. Shoji, M. Takahashi, T. Tsuchizawa, T. Watanabe, J. Takahashi, and S. Itabashi, "Four-wave mixing in silicon wire waveguides," Opt. Express **13**(12), 4629–4637 (2005), http://www.opticsinfobase.org/oe/abstract.cfm?URI=OPEX-13-12-4629.
11. Q. Lin, J. Zhang, P. M. Fauchet, and G. P. Agrawal, "Ultrabroadband parametric generation and wavelength conversion in silicon waveguides," Opt. Express **14**(11), 4786–4799 (2006), http://www.opticsinfobase.org/oe/abstract.cfm?URI=OPEX-14-11-4786.
12. X. Zhang, S. Gao, and S. He, "Optimal design of a silicon-on-insulator nanowire waveguide for broadband wavelength conversion," Prog. Electromagn. Res. **89**, 183–198 (2009).

#126567 - $15.00 USD Received 6 Apr 2010; revised 10 May 2010; accepted 10 May 2010; published 20 May 2010

13. A. C. Turner, C. Manolatou, B. S. Schmidt, M. Lipson, M. A. Foster, J. E. Sharping, and A. L. Gaeta, "Tailored anomalous group-velocity dispersion in silicon channel waveguides," Opt. Express **14**(10), 4357–4362 (2006), http://www.opticsinfobase.org/oe/abstract.cfm?URI=OPEX-14-10-4357.
14. A. C. Turner-Foster, M. A. Foster, R. Salem, A. L. Gaeta, and M. Lipson, "Frequency conversion over two-thirds of an octave in silicon nanowaveguides," Opt. Express **18**(3), 1904–1908 (2010), http://www.opticsinfobase.org/oe/abstract.cfm?URI=OPEX-18-3-1904.
15. X. Liu, W. M. J. Green, X. Chen, I.-W. Hsieh, J. I. Dadap, Y. A. Vlasov, and R. M. Osgood, Jr., "Conformal dielectric overlayers for engineering dispersion and effective nonlinearity of silicon nanophotonic wires," Opt. Lett. **33**(24), 2889–2891 (2008).

1. Introduction

Wavelength converter is a key signal processing component to increase the versatility in wavelength division multiplexing (WDM) networks and to avoid the network block when multiple channels at the same wavelength are routed at the same port [1]. Current state of the art on wavelength converters mainly focuses on the conversion between channels pertinent to long-haul communication systems utilizing dense WDM channels in 1550-nm window. However, the network nodes interfacing fiber-to-the-premises access systems resort to course WDM systems utilizing both 1310-nm and 1550-nm windows [2]. To ensure the system performance, broadband wavelength converters are necessary to cover this wide wavelength range including both 1310-nm and 1550-nm bands. Up to date, many efforts have been made to enhance the bandwidth of wavelength converters based on wave mixing such as designing special structures in ferroelectric crystals [3] and adopting short ultra-highly nonlinear fibers [4]. In a further study, two-pump wave mixing technology has been utilized to enhance the bandwidth. For example, the conversion bandwidth has been enhanced by using cascaded three-wave mixing with two pumps in periodically poled crystals [5]. Also a two-pump nondegenerate four-wave mixing (FWM) in optical fibers has also been used to convert signals from 1550 nm to 1310 nm [6].

Intrinsic high nonlinearity of silicon and its potential for full optoelectronic integration attracted researchers to develop novel silicon-based chip scale nonlinear devices. Some schemes have been theoretically proposed or experimentally demonstrated for wavelength conversion in silicon waveguides [7–10]. In particular, the dispersion profiles of the silicon waveguides have been optimized to enhance the conversion bandwidth [11–15]. In this paper, we present and demonstrate, for the first time to our best knowledge, an ultra-broadband wavelength conversion based on two-pump nondegenerate FWM in silicon waveguides by setting one pump near the signal and scanning the other pump to eliminate the phase mismatch. Total conversion bandwidth is estimated to reach >500 nm and it can provide a feasible approach to realize wavelength conversion between 1300 nm and 1800 nm. Moreover, two idlers can be generated simultaneously and hence this scheme has the one-to-two conversion ability.

2. Principle

Figure 1 illustrates the proposed ultra-broadband wavelength conversion utilizing nondegenerate FWM to create a dual replica of an optical signal. To achieve the phase match over a broad wavelength range, the first pump P_1 is set near the signal wave S. The second pump P_2 is set near the frequencies at which the idlers are desired. When the involved pump and signal waves are injected into a silicon waveguide, two typical nondegenerate FWM processes occur and two idlers are generated, which are denoted as I_1 and I_2. As shown in Fig. 1, the frequencies of the two idlers are written as $f_{I1} = f_S + f_{P2} - f_{P1}$ and $f_{I2} = f_{P1} + f_{P2} - f_S$ according to the energy conservation law, where $f_{P1,P2,S,I1,I2}$ are the frequencies of the involved waves. Correspondingly, the phase mismatches for the two FWM processes can be expressed as

$$\kappa_1 = \beta_{P1} - \beta_S + \beta_{I1} - \beta_{P2} + (2\pi n_2 f_{P1} / c) I_{P1} + (2\pi n_2 f_{P2} / c) I_{P2} \quad (1)$$

$$\kappa_2 = \beta_S - \beta_{P1} + \beta_{I2} - \beta_{P2} + (2\pi n_2 f_{P1} / c) I_{P1} + (2\pi n_2 f_{P2} / c) I_{P2} \quad (2)$$

#126567 - $15.00 USD Received 6 Apr 2010; revised 10 May 2010; accepted 10 May 2010; published 20 May 2010

where $\beta_{P1,P2,S,I1,I2}$ are the wave numbers of the corresponding signals, n_2 is the nonlinear index coefficient, and $I_{P1,P2}$ are the pump intensities. As shown in Fig. 1, the first pump P_1 is very close to the signal S and the small frequency spacing between the first pump and the signal is denoted as Δf. Due to the law of conservation of energy in FWM processes, the idlers I_1 and I_2 will also have frequency spacing $\pm \Delta f$ between the second pump P_2. Therefore, the wave number differences between the adjacent interacting waves β_S and β_{P1} (also $\beta_{I1,I2}$ and β_{P2}) are small regardless of the actual wavelength of P_2. As long as Δf is small enough to minimize $\beta_{P1} - \beta_S$, the total phase mismatches will be low for high-efficiency wavelength conversion over an ultra-broad conversion bandwidth.

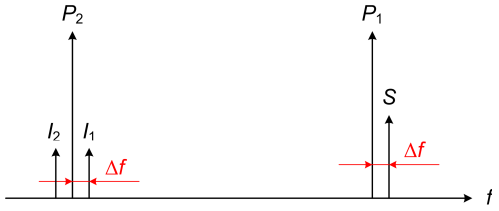

Fig. 1. Principle of ultra-broadband one-to-two wavelength conversion based on nondegenerate FWM.

In above analysis, the waveguide dispersion profile is not taken into account. In fact, the influence of waveguide dispersion will be slight and the phase mismatch can be controlled to be low once the first pump is set close to the signal according to Eqs. (1) and (2). As a result, ultra-broad bandwidth can be achieved in spite of the waveguide characteristics, which is quite convenient for realizing practical ultra-broadband wavelength converters.

3. Numerical simulation

Proof-of-concept simulations are performed by using silicon waveguides with different geometries and hence different dispersion profiles. Particular waveguide parameters are derived for four silicon waveguides with dimensions of 300 × 500 nm^2, 300 × 650 nm^2, 285 × 650 nm^2, and 3 × 3 μm^2 by using beam propagation method. In these simulations, the linear loss of the silicon waveguides is assumed to be 0.7 cm^{-1}, the two-photon absorption coefficient is 0.8 cm/GW, the free carrier lifetime is 2 ns, and the nonlinear index coefficient is 9×10^{-18} m^2/W. Both of the incident pump intensities are assumed to be 100 mW/μm^2 and the signal intensity is 10 mW/μm^2. According to the ITU WDM channel grid, the first pump P_1 is set at 1543.73 nm (Ch42) and the signal S is at 1542.94 nm (Ch43). By scanning the wavelength of the second pump P_2, Fig. 2 shows the phase mismatch and the corresponding conversion efficiency, which is defined as the ratio of the generated idler power with respect to the incident signal power: $\eta = P_{I1,I2\text{-}out}/P_{S\text{-}in}$. The phase mismatch and efficiency for the idler I_1 are shown in Figs. 2(a) and 2(b). It is shown that the phase mismatch can be controlled to be within ± 2 cm^{-1} for a wavelength region of >550 nm in 17-mm-long silicon waveguides with different dimensions. As a result, the conversion response exhibits an ultra-broad bandwidth. The 3-dB bandwidth is calculated from Fig. 2(b) to be subsequently 630 nm, 604 nm, 535 nm, and 558 nm for the above mentioned waveguides, respectively. For the idler I_2 shown in Fig. 2(c), the phase mismatch almost has an opposite sign compared with the idler I_1 as the linear phase mismatches in Eqs. (1) and (2) are approximately opposite and the intensity-induced phase mismatches are small. Therefore, the conversion response of the idler I_2 in Fig. 2(d) is almost the same as that of the idler I_1 in Fig. 2(b) and an ultra-broad bandwidth can also be predicted, that is, the one-to-two ultra-broadband wavelength conversion can be achieved using this method.

As demonstrated above, the realization of the ultra-broad bandwidth depends on the small frequency spacing Δf between the signal S and the first pump P_1. If the frequency spacing is increased, the differences between β_S and β_{P1} (also $\beta_{I1,I2}$ and β_{P2}) will also increase. As a result, the phase mismatch will increase rapidly and the conversion bandwidth will decrease.

#126567 - $15.00 USD Received 6 Apr 2010; revised 10 May 2010; accepted 10 May 2010; published 20 May 2010

By keeping the pump P_1 at 1543.73 nm (Ch42) and tuning the signal S from 1542.94 nm (Ch43) to 1540.56 nm (Ch46) in the 3 × 3 μm^2 waveguide, the influence of the frequency spacing can be observed, as shown in Fig. 3, where the idler I_1 is taken as the example. From Fig. 3(a), one can find that the phase mismatch is enlarged when the signal S goes far away from the pump P_1, and the corresponding conversion bandwidth is reduced dramatically. As shown in Fig. 3(b), the 3-dB bandwidth reduces from 558 nm to 159 nm for the signals at ITU WDM channels of Ch43-46 (558 nm, 309 nm, 210 nm, and 159 nm), respectively.

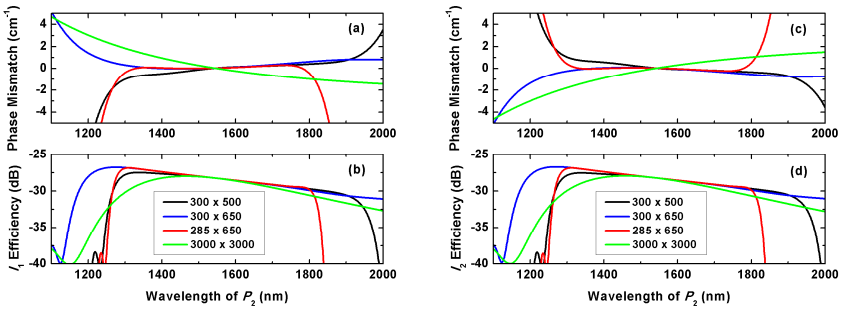

Fig. 2. Calculated phase mismatch and conversion efficiency for the two generated idlers in 300 × 500 nm^2, 300 × 650 nm^2, 285 × 650 nm^2, and 3 × 3 μm^2 silicon waveguides. (a) I_1 phase mismatch; (b) I_1 conversion efficiency; (c) I_2 phase mismatch; (d) I_2 conversion efficiency.

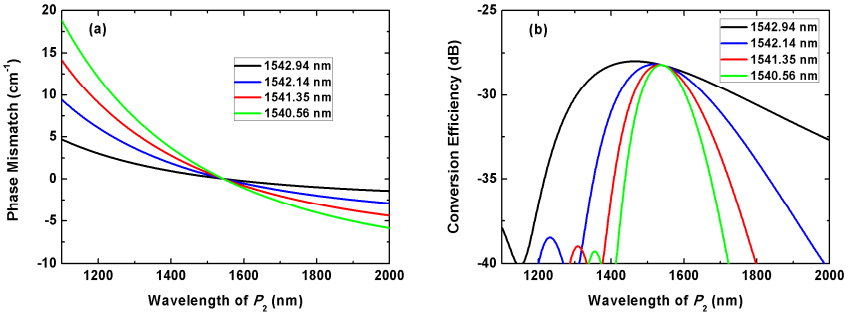

Fig. 3. Simulation results of (a) the phase mismatch and (b) the conversion efficiency of the idler I_1 for different signal wavelengths as the pump P_2 scans and the pump P_1 is fixed at 1543.73 nm.

4. Experimental demonstration

Theoretical predictions are tested at telecommunication wavelengths in the experimental setup shown in Fig. 4. The first pump P_1 and the signal S are produced by two continuous-wave tunable lasers (Santec ECL-200). They are coupled together via a 50/50 coupler and amplified by a high-power erbium-doped fiber amplifier (Amonics AEDFA-C-33-R). After eliminating the amplified spontaneous emission noise using a tunable band-pass filter (its bandwidth is about 2 nm and can let P_1 and S pass simultaneously), the first pump P_1 and the signal S are coupled into a 17-mm-long silicon waveguide with 5 μm^2 effective mode area together with the second pump P_2, which is produced by another continuous-wave tunable laser (Santec ECL-210), through a 70/30 coupler. In the silicon waveguide, the two FWM processes analyzed in section 2 occur and two idlers I_1 and I_2 are generated. They are observed using an optical spectrum analyzer (Ando AQ6317B). By scanning the second pump P_2, the signal S can be converted to the idlers in different wavelength regions.

#126567 - $15.00 USD Received 6 Apr 2010; revised 10 May 2010; accepted 10 May 2010; published 20 May 2010

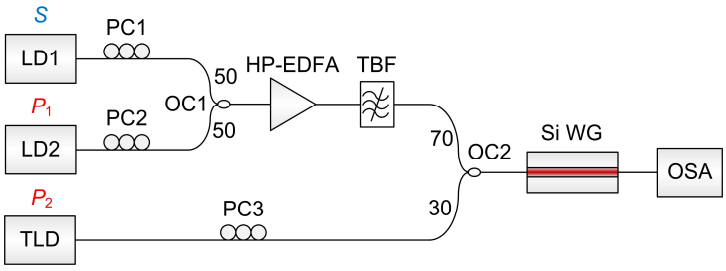

Fig. 4. Experimental setup for ultra-broadband one-to-two wavelength conversion.

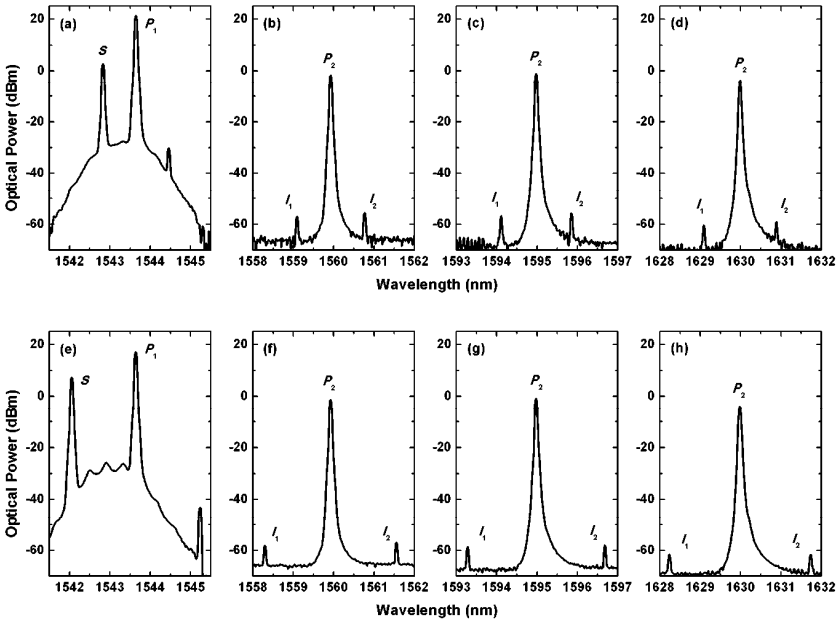

Fig. 5. Measured optical spectra for the signal at 1542.83 nm or 1542.05 nm when the pump P_1 is set at 1543.64 nm. (a) The pump P_1 and the 1542.83-nm signal; (b)-(d) the pump P_2 and the generated idlers $I_{1,2}$ when the pump P_2 is at 1560 nm, 1595 nm, and 1630 nm corresponding to (a); (e) the pump P_1 and the 1542.05-nm signal; (f)-(h) the pump P_2 and the generated idlers $I_{1,2}$ when the pump P_2 is at 1560 nm, 1595 nm, and 1630 nm corresponding to (e).

The measured optical spectra are shown in Fig. 5, where the first pump P_1 is set at 1543.64 nm and the signal is set at 1542.83 nm [Figs. 5(a)–5(d)] or 1542.05 nm [Figs. 5(e)–5(h)], whose wavelength spacing to the pump P_1 is around 0.8 nm or 1.6 nm. For the 1542.83-nm signal, Fig. 5(a) shows the spectra of the first pump P_1 and the signal S. The spectra of the second pump P_2 and the generated idlers $I_{1,2}$ are shown in Figs. 5(b)–5(d) when P_2 is tuned to 1560nm, 1595 nm, and 1630 nm, respectively. It is noticeable that the generated idler powers are almost unchanged when scanning the wavelength of the pump P_2, which indicates an ultra-broad conversion bandwidth. Unfortunately, the tunable laser we used for the pump P_2 in our experiment has a limited tuning range from 1530 nm to 1630 nm and the FWM effects cannot be measured for the pump P_2 beyond 1630 nm. Figures 5(e)–5(h) show the spectra for the 1542.05-nm signal, which are quite similar to Figs. 5(a)–5(d) expect for the enlargement of wavelength spacing between the two idlers and the second pump. Moreover, the idler powers are a little smaller than those for the 1542.83-nm signal because a larger phase mismatch is introduced when the signal S moves away from the pump P_1.

#126567 - $15.00 USD Received 6 Apr 2010; revised 10 May 2010; accepted 10 May 2010; published 20 May 2010

In order to quantitatively evaluate the performance of the proposed wavelength conversion, the conversion efficiency is measured. For the convenience of comparison, we introduce a unit conversion efficiency to eliminate the effect of the pump powers, which is defined as $\eta_{unit} = \eta_{appro}/(P_{P1}P_{P2})$ and the approximate conversion efficiency η_{appro} is the ratio of the output idler power with respect to the output signal power: $\eta_{appro} = P_{I1,I2\text{-}out}/P_{S\text{-}out}$. With such definitions, Fig. 6 shows the unit conversion efficiency calculated from the measured output FWM spectra. As indicated in Fig. 6, the unit conversion efficiency for each idler (I_1 or I_2) varies very slight when the wavelength of pump P_2 changes. The experiment data are fitted and the efficiency difference within 100 nm (1550-1650 nm) is only 0.8 dB and 1.5 dB for the 0.8-nm and 1.6-nm wavelength spacing respectively. The entire 3-dB bandwidth cannot be measured due to the tuning range of the pump laser. However, the prediction from the measured efficiency data agrees well with the theoretical analysis and the ultra-broadband wavelength conversion performance can also be verified.

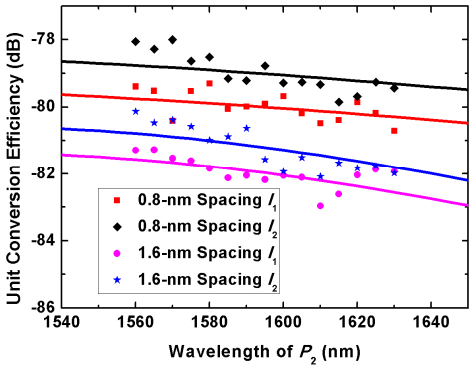

Fig. 6. Measured unit conversion efficiencies of the two idlers and their fitting curves as the pump P_2 scans for the 1542.83-nm and 1542.05-nm signals that have 0.8-nm and 1.6-nm spacing with the pump P_1.

5. Conclusion

The ultra-broadband one-to-two wavelength conversion has been theoretically presented and experimentally demonstrated in silicon waveguides using two-pump nondegenerate FWM where one pump is set near the signal and the other pump scans. Simulation results show the conversion bandwidth is >500 nm when the signal and the pump occupy two adjacent ITU WDM channels and have a wavelength spacing of 0.8 nm. The bandwidth is insensitive to the dispersion profile of the waveguide. The wavelength conversion has been experimentally realized for two signals whose wavelengths are 0.8 nm and 1.6 nm apart from the pump. Two generated idlers from the two FWM processes have been observed and experimental results agree well with the simulations.

Acknowledgements

This work was supported in part by the National Natural Science Foundation of China (Grant Nos. 60708006 and 60978026), the Specialized Research Fund for the Doctoral Program of Higher Education of China (Grant No. 20070335118), and the Zhejiang Provincial Natural Science Foundation of China (Grant No. Y1090379).

#126567 - $15.00 USD Received 6 Apr 2010; revised 10 May 2010; accepted 10 May 2010; published 20 May 2010